

# Synthesis of 3,4-Diphenyl-Substituted Poly(Thienylene Vinylene), Low-Band-Gap Polymers via the Dithiocarbamate Route

A. Henckens,<sup>†,‡</sup> K. Colladet,<sup>†</sup> S. Fourier,<sup>†</sup> T. J. Cleij,<sup>†</sup> L. Lutsen,<sup>‡</sup> J. Gelan,<sup>†</sup> and D. Vanderzande<sup>\*,†,‡</sup>

Limburgs Universitair Centrum, Institute for Materials Research (IMO), Universitaire Campus, Building D, B-3590 Diepenbeek, Belgium, and IMEC, Division IMOMECE, Universitaire Campus, Wetenschapspark 1, B-3590 Diepenbeek, Belgium

Received October 6, 2004; Revised Manuscript Received October 29, 2004

**ABSTRACT:** It has been demonstrated that the dithiocarbamate precursor route is a suitable pathway towards poly(thienylene vinylene) (PTV)-type low-band-gap polymers. Two particular dithiocarbamate precursor polymers and the corresponding conjugated polymers, poly(3,4-diphenyl-2,5-thienylene vinylene) and poly(3,4-bis(4-butylphenyl)-2,5-thienylene vinylene), have been studied. The introduction of butyl side chains in the latter leads to excellent solubility in common organic solvents. Both polymers have been prepared in a straightforward manner and in good yield. The thermal conversion of the precursor polymers into the conjugated structure was studied with in situ FT-IR and UV–vis spectroscopy. Also, with the latter technique, the band gap was determined and the thermochromic effect was studied and compared with the unsubstituted PTV. The HOMO and LUMO levels of the polymers were determined from UV–vis and electrochemical measurements.

## Introduction

Since their discovery, conjugated polymers attract continuing interest as a result of their suitability in a broad range of application fields, such as batteries, electroluminescent devices,<sup>1</sup> field-effect transistors,<sup>2</sup> and photovoltaics.<sup>3</sup> For the latter two applications, poly(thienylene vinylene) (PTV) has already proven to be an interesting conjugated polymer with a high conductivity.<sup>4–7</sup> In addition, PTV has a band gap of about 1.7 eV and, as a result, can be regarded as a low-band-gap polymer. Furthermore, an advantage of PTV and its derivatives is their high absorption in the visible range of the spectrum, making them excellent candidates for photovoltaic applications.<sup>8,9</sup> However, the limited processability of unsubstituted PTV is troublesome. Hence, our current research efforts focus on substituted PTV derivatives with improved properties.

An example of such a substituted PTV derivative is poly(3,4-diphenyl-2,5-thienylene vinylene) (DP-PTV). It is anticipated that, in this particular derivative, the steric hindrance of the reactive 3 and 4 positions by the two phenyl rings will lead to a higher stability than its unsubstituted analogue, which is advantageous for applications. Additionally, it is expected that the introduction of phenyl substituents will lead to a decrease in the band gap, yielding an even broader absorption of visible light, which would increase the applicability of this class of conjugated materials in photovoltaic applications. Despite these promising features, surprisingly only limited reports exist on the synthesis and use of DP-PTV. These few reports focus on the modification of the optical properties of DP-PTV via near-field optical microscopy.<sup>10–12</sup> However, the DP-PTV employed in those studies was synthesized via the chlorine precursor

or Gilch route,<sup>13,14</sup> a route which inherently is characterized by gel formation and the instability of the precursor polymer. Hence, a pathway toward DP-PTV via a more suitable route is desirable. Earlier, we reported on the synthesis of PTV via the dithiocarbamate route.<sup>7</sup> On the basis of these successful results, the dithiocarbamate route has been chosen as the method of choice to obtain DP-PTV. In this article, the synthesis of DP-PTV via this dithiocarbamate route is described. Furthermore, three different routes toward the required bischloromethylthiophene derivatives have been compared to find the most suitable synthetic procedure to further increase the accessibility of DP-PTV for applications.

One of the major factors causing the limited processability of PTV is the general insolubility of this type of polymers. This problem can be partially circumvented by working via a soluble precursor polymer. One of the first examples of the use of such an indirect method to obtain 3,4-substituted PTV derivatives is the bis-sulfoxide precursor route.<sup>15</sup> In this article, we have demonstrated the viability of working via a soluble precursor polymer for DP-PTV. Notwithstanding, the synthesis of a soluble, conjugated PTV derivative could be a substantial additional advantage. We have tackled this problem by the introduction of additional alkyl side chains onto the DP-PTV. Therefore, this article not only reports on the successful synthesis of DP-PTV but also reports on the straightforward preparation of a novel soluble derivative of DP-PTV, poly(3,4-bis(4-butylphenyl)-2,5-thienylene vinylene). Both polymers have been fully characterized, and their electronic properties have been evaluated using optical spectroscopy and electrochemistry. In addition, the elimination process has been studied in more detail using temperature-dependent FT-IR, as well as UV–vis spectroscopy.

## Experimental Section

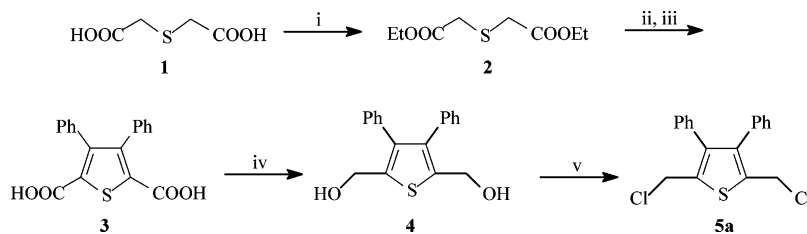
**General.** Unless otherwise stated, all reagents and chemicals were obtained from commercial sources (Acros and Ald-

\* Author to whom correspondence should be addressed. Phone: +32 (0)11 26 83 21. Fax: +32 (0)11 26 83 01. E-mail: dirk.vanderzande@luc.ac.be.

<sup>†</sup> Limburgs Universitair Centrum, Institute for Materials Research (IMO), Universitaire Campus.

<sup>‡</sup> IMEC, Division IMOMECE, Universitaire Campus.

**Scheme 1. Synthetic Route 1 toward the Synthesis of 3,4-Diphenyl-2,5-bis(chloromethyl)thiophene 5a:** i) EtOH; ii) NaOH, EtOH; iii) PhC(O)C(O)Ph; iv) LiAlH<sub>4</sub>, THF; v) SOCl<sub>2</sub>, THF



rich) and used without further purification. Tetrahydrofuran (THF) and CH<sub>3</sub>CN were dried by distillation from sodium/benzophenone and CaH<sub>2</sub>, respectively.

NMR spectra were recorded with a Varian Inova 300 spectrometer at 300 MHz for <sup>1</sup>H NMR and at 75 MHz for <sup>13</sup>C NMR using a 5 mm probe. Gas chromatography/mass spectrometry (GC/MS) analyses were carried out with TSQ-70 and Voyager mass spectrometers (Thermoquest); the capillary column was a Chrompack Cpsil5CB or Cpsil8CB. Analytical size exclusion chromatography (SEC) was performed using a Spectra series P100 (Spectra Physics) pump equipped with two mixed-B columns (10 μm, 2 cm × 30 cm, Polymer Labs) and a refractive index detector (Shodex) at 70°C. A DMF solution of oxalic acid (1.1 × 10<sup>-3</sup> M) was used as the eluent at a flow rate of 1.0 mL/min. Molecular weight distributions are given relative to polystyrene standards. FT-IR spectra were collected with a Perkin-Elmer Spectrum One FT-IR spectrometer (nominal resolution 4 cm<sup>-1</sup>, summation of 16 scans). UV-vis spectroscopy was performed on a VARIAN CARY 500 UV-vis-NIR spectrophotometer (scan rate: 600 nm/min). Samples for temperature-dependent thin-film FT-IR and UV-vis characterization were prepared by spin-coating the precursor polymer from a CHCl<sub>3</sub> solution (10 mg/mL) onto NaCl disks at 500 rpm or quartz disks at 700 rpm. The disks were heated in a Harrick high-temperature cell (heating rate: 2 °C/min), which was positioned in the beam of either the FT-IR or the UV-vis spectrometer to allow in-situ measurements. Spectra were taken continuously under a continuous flow of N<sub>2</sub> during which the samples were in direct contact with the heating element. Fluorescence spectra were obtained with a Perkin-Elmer LS-5B luminescence spectrometer.

Thin-film electrochemical properties were measured with an Eco Chemie Autolab PGSTAT 20 potentiostat/galvanostat using a conventional three-electrode cell (electrolyte: 0.1 mol/L LiClO<sub>4</sub> in anhydrous CH<sub>3</sub>CN) with an Ag/Ag<sup>+</sup> reference electrode (0.01 mol/L AgNO<sub>3</sub>, 0.1 mol/L LiClO<sub>4</sub> and CH<sub>3</sub>CN), a platinum counter electrode, and an indium-tin oxide (ITO) coated glass substrate as working electrode. Cyclic voltammograms were recorded at 50 mV/s under N<sub>2</sub> atmosphere, and all potentials were referenced using a known standard (ferrocene/ferrocinium, 0.099 V vs Ag/Ag<sup>+</sup>). Precursor polymer **13a** was spin-coated from a CHCl<sub>3</sub> solution (5 mg/mL) onto the ITO working electrode and subsequently converted to the conjugated polymer **14a** by thermal treatment under a continuous flow of N<sub>2</sub>. Polymer **14b** was directly spin-coated from a CHCl<sub>3</sub> solution (5 mg/mL) onto the ITO working electrode. Solution electrochemistry was performed using the same setup (electrolyte: 0.1 mol/L TBAPF<sub>6</sub> in anhydrous CH<sub>2</sub>Cl<sub>2</sub>) and a Pt working electrode.

**Synthesis. Diethyl Thiodiacetate (2).** A mixture of thiodiglycolic acid (10 g, 66.7 mmol), absolute ethanol (30 mL), and 3 drops of concentrated H<sub>2</sub>SO<sub>4</sub> as a catalyst was allowed to react overnight at reflux temperature. After cooling, an extraction with CHCl<sub>3</sub> (3 × 50 mL) was performed and the combined organic layers were dried over MgSO<sub>4</sub>. After evaporation of the solvent, a colorless liquid was obtained (12.36 g, 90% yield); <sup>1</sup>H NMR (CDCl<sub>3</sub>): 4.17 (q, 4H), 3.60 (s, 4H), 1.26 (t, 6H); MS (EI, *m/e*): 206 (M<sup>+</sup>), 161 (M<sup>+</sup> - OEt), 133 (M<sup>+</sup> - COOEt), 104 (M<sup>+</sup> - COOEt - Et).

**3,4-Diphenylthiophene-2,5-dicarboxylic Acid (3).** To a mixture of **2** (2 g, 9.71 mmol) and benzil (2.04 g, 9.71 mmol) in methanol (15 mL), NaOMe (1.57 g, 29.1 mmol) was added

as a solid. The mixture was stirred at ambient temperature for 3 days. After addition of water, the alcohol was evaporated. The formed solid (benzil) was filtered off, and the filtrate was acidified with HCl, upon which **3** precipitated. After filtration, a white solid was obtained (2.02 g, 64% yield); <sup>1</sup>H NMR (CD<sub>3</sub>OD): 7.12–7.05 (m, 6H), 7.02–6.93 (m, 4H); DIP MS (CI, *m/e*): 325 (M<sup>+</sup> + 1), 281 (M<sup>+</sup> + 1 - COO).

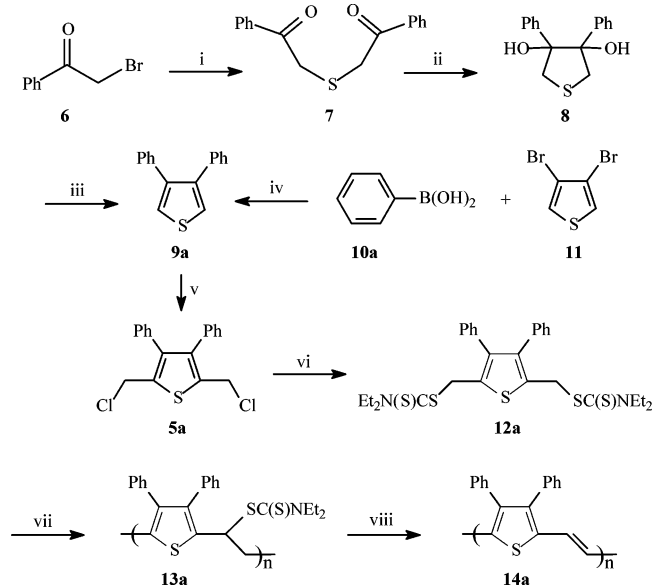
**3,4-Diphenyl-2,5-bis(chloromethyl)thiophene (5a)** via Method 1 (cf. Scheme 1). A solution of **3** (1 g, 3.09 mmol) in THF (20 mL) was added to a suspension of LiAlH<sub>4</sub> (0.35 g, 9.26 mmol) in THF (10 mL) at 0 °C. The mixture was allowed to warm to ambient temperature, was stirred for 2 h, and then was heated to reflux temperature for an additional 2 h. The reaction mixture was quenched by the addition of HCl (1 M) until the reaction mixture was neutral. After extraction with CHCl<sub>3</sub> (3 × 20 mL), the combined organic layers were dried over MgSO<sub>4</sub> and the solvent was evaporated. The alcohol formed in this way was used without further purification [DIP MS (EI, *m/e*): 296 (M<sup>+</sup>), 279 (M<sup>+</sup> - OH), 249]. To a solution of the alcohol in THF (5 mL), thionyl chloride (0.5 mL, 6.790 mmol) was added dropwise at 0°C. The mixture was stirred at room temperature for 2 h, after which the mixture was neutralized with NaHCO<sub>3</sub>. After extraction with CHCl<sub>3</sub> (3 × 20 mL), the combined organic layers were dried over MgSO<sub>4</sub> and the solvent was evaporated giving a white solid (430 mg, 42% yield); <sup>1</sup>H NMR (CDCl<sub>3</sub>): 7.24–7.21 (m, 6H), 7.08–7.05 (m, 4H), 4.67 (s, 4H); MS (EI, *m/e*): 332 (M<sup>+</sup>), 297 (M<sup>+</sup> - Cl), 261 (M<sup>+</sup> - 2 Cl). Upon purification by column chromatography (silica, CHCl<sub>3</sub>/hexane 3:7, 6:4, 1:0, gradual enrichment of CHCl<sub>3</sub>) of **5a**, some degradation occurred as a result of its instability.

**1,5-Diphenyl-3-thiapentane-1,5-dione (7).** A solution of Na<sub>2</sub>S·9H<sub>2</sub>O (10.5 g, 43.6 mmol) in water (50 mL) was added to a solution of 2-bromoacetophenone (15 g, 87.2 mmol) in acetone (70 mL) over a period of 1 h at 0 °C. The mixture was allowed to warm to ambient temperature and was stirred for an additional hour. After dilution with water (100 mL), an extraction with CHCl<sub>3</sub> (3 × 50 mL) was performed and the combined organic layers were dried over MgSO<sub>4</sub>. Evaporation of the solvent gave a yellow solid (10.0 g, 42% yield); <sup>1</sup>H NMR (CDCl<sub>3</sub>): 7.97 (dd, 4H), 7.60–7.55 (tt, 2H), 7.48–7.43 (t, 4H), 3.97 (s, 4H); MS (EI, *m/e*): 270 (M<sup>+</sup>), 237, 165, 105.

**3,4-Diphenylthiolane-3,4-diol (8).** To a well-stirred suspension of Zn powder (7.22 g, 111 mmol) and **7** (5 g, 18.5 mmol) in THF (60 mL) under argon atmosphere and at -18 °C, TiCl<sub>4</sub> (6.1 mL, 55.6 mmol) was added dropwise over a period of 3 h. The mixture was allowed to warm to 0 °C and stirred for 3 h at 0–15 °C. The reaction was quenched by addition of crushed ice (60 g), and the pH of the solution was brought to 9 by adding a saturated aqueous solution of K<sub>2</sub>CO<sub>3</sub>. Dichloromethane (150 mL) was added, and the mixture was stirred overnight, after which it was filtered over a large glass filter on which a layer of Celite was placed. The organic layer of the filtrate was washed with water (5 × 250 mL) and dried over MgSO<sub>4</sub>, and evaporation of the solvent gave a brown partially crystallized solid (4.50 g, 89% yield); <sup>1</sup>H NMR (CDCl<sub>3</sub>): 7.19–7.05 (m, 10H), 3.62 (d, 2H), 3.15 (d, 2H); MS (EI, *m/e*): 236 (M<sup>+</sup> - H<sub>2</sub>O), 152, 120, 105.

**3,4-Diphenylthiophene (9a).** Compound **9a** was prepared via two different synthetic methods (vide infra). (*Method a*) A mixture of **8** (4.5 g, 16.5 mmol) and TsOH·H<sub>2</sub>O (1.57 g, 8.27 mmol) in benzene (30 mL) was heated at reflux temperature for 4 h during which the azeotropically formed water was

**Scheme 2. Synthetic Routes 2 and 3 toward the Synthesis of 3,4-Diphenyl-2,5-bis(chloromethyl)thiophene 5a, as Well as the Synthesis of the Dithiocarbamate Monomer 12a and Polymers 13a and 14a:** i)  $\text{Na}_2\text{S}\cdot 9\text{H}_2\text{O}$ ,  $\text{Me}_2\text{CO}/\text{H}_2\text{O}$ ; ii)  $\text{TiCl}_4$ , Zn, THF; iii)  $\text{TsOH}\cdot\text{H}_2\text{O}$ , PhH; iv)  $\text{Pd}(\text{PPh}_3)_4$ , KF, Toluene/ $\text{H}_2\text{O}$ ; v)  $\text{CH}_2\text{O}$ , HCl,  $\text{Ac}_2\text{O}$ ; vi)  $\text{NaSC}(\text{S})\text{NEt}_2\cdot 3\text{H}_2\text{O}$ , MeOH; vii) LDA, THF; viii)  $\Delta T$



removed using a Dean–Stark apparatus. The obtained mixture was washed with an aqueous solution of  $\text{NaHCO}_3$  (5%, 30 mL) and water (30 mL), after which it was dried over  $\text{MgSO}_4$  and the solvents were removed by evaporation. The crude mixture was purified by column chromatography (silica,  $\text{CHCl}_3/n$ -hexane 1:4), and a white solid was obtained (3.0 g, 77% yield).

(Method b) Phenylboronic acid (5 g, 41.0 mmol), 3,4-dibromothiophene (2.14 g, 8.85 mmol), and KF (2.10 g, 36.2 mmol) were dissolved in water (40 mL) and toluene (40 mL).  $\text{Pd}(\text{PPh}_3)_4$  (730 mg) was added as a catalyst. After the mixture was refluxed for 18 h, an extraction with  $\text{CHCl}_3$  ( $3 \times 50$  mL) was performed and the combined organic phases were dried over  $\text{MgSO}_4$ . The crude reaction product was purified by column chromatography (silica,  $n$ -hexane), and a white solid was obtained (1.6 g, 77% yield);  $^1\text{H NMR}$  ( $\text{CDCl}_3$ ): 7.30 (s, 2H), 7.25–7.21 (m, 6H), 7.19–7.16 (m, 4H); MS (EI,  $m/e$ ): 236 ( $\text{M}^+$ ).

3,4-Diphenyl-2,5-bis(chloromethyl)thiophene (5a) via Methods 2 and 3 (cf. Scheme 2). To a mixture of paraformaldehyde (343 mg, 11.4 mmol) and 9a (1 g, 4.24 mmol), concentrated HCl (2.35 g, 24.2 mmol) and acetic anhydride (4.32 g, 42.4 mmol) were added dropwise under  $\text{N}_2$  atmosphere at  $0^\circ\text{C}$ . The mixture was heated at  $70^\circ\text{C}$  for 4.5 h, after which a cold ( $0^\circ\text{C}$ ) saturated aqueous solution of sodium acetate (10 mL) and a 25% aqueous solution of sodium hydroxide (10 mL) were added. The mixture was extracted with  $\text{CHCl}_3$  ( $3 \times 50$  mL) and dried over  $\text{MgSO}_4$ . After evaporation of the solvents, a light brown solid was obtained (1.38 g, 98% yield);  $^1\text{H NMR}$  ( $\text{CDCl}_3$ ): 7.24–7.21 (m, 6H), 7.08–7.05 (m, 4H), 4.67 (s, 4H); MS (EI,  $m/e$ ): 332 ( $\text{M}^+$ ), 297 ( $\text{M}^+ - \text{Cl}$ ), 261 ( $\text{M}^+ - 2\text{Cl}$ ).

3,4-Diphenylthiophene-2,5-diylbismethylene-*N,N*-diethylthiocarbamate (12a). A mixture of 5a (3 g, 8.89 mmol) and sodium diethylthiocarbamate trihydrate (4.6 g, 20.4 mmol) in 10 mL of methanol was stirred for 3 h at ambient temperature. Subsequently, the mixture was extracted with diethyl ether ( $3 \times 50$  mL) and dried over  $\text{MgSO}_4$ . The crude reaction mixture was purified by column chromatography (silica,  $n$ -hexane/ $\text{CHCl}_3$  3:7), after which the dithiocarbamate monomer was obtained as a white solid (3.47 g, 70% yield);  $^1\text{H NMR}$  ( $\text{CDCl}_3$ ): 7.24–7.14 (m, 6H), 7.03–7.00 (m, 4H), 4.62 (s, 4H), 4.01 (q,  $J = 7.2$  Hz, 4H), 3.69 (q,  $J = 7.2$  Hz, 4H), 1.26 (2t,  $J = 7.2$  Hz, 12H);  $^{13}\text{C NMR}$  ( $\text{CDCl}_3$ ): 194.22 (2C),

**Table 1. Polymerization Results for Monomers 12a (entry 1–3) and 12b (entry 4)**

entry	polymerization temperature ( $^\circ\text{C}$ )	yield (%)	$M_w$ ( $\times 10^{-3}$ )	PD
1	0	20	50.4	1.4
2	-78	40	29.8	1.2
3	-78 $\rightarrow$ 0	35	24.6	1.2
4	-78	38	16.2, 3.3 <sup>a</sup>	1.2, 1.1 <sup>a</sup>

<sup>a</sup> Bimodal molecular weight distribution.

141.14 (2C), 135.33 (2C), 133.39 (2C), 129.99 (4C), 127.82 (4C), 126.77 (2C), 49.31 (2C), 46.63 (2C), 35.82 (2C), 12.39 (2C), 11.43 (2C).

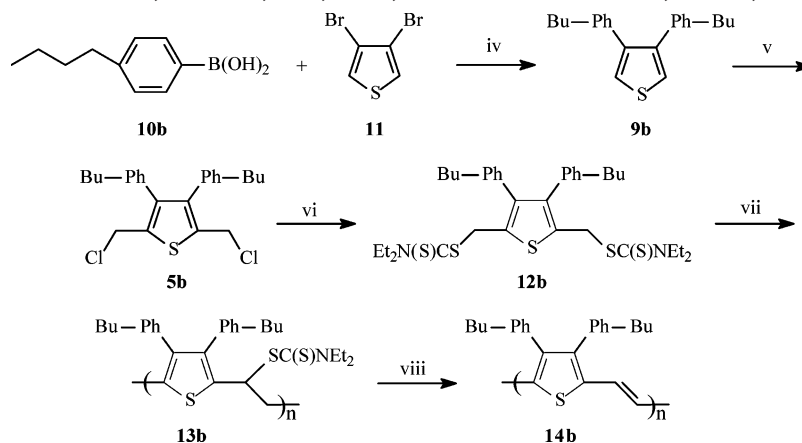
3,4-Bis(4-butylphenyl)thiophene (9b). Compound 9b was obtained in an analogous way to that described for 9a (method b), starting from 4-butylphenylboronic acid (2.5 g, 14.0 mmol) and 3,4-dibromothiophene (0.885 g, 3.66 mmol). A colorless oil was obtained (730 mg, 60% yield);  $^1\text{H NMR}$  ( $\text{CDCl}_3$ ): 7.26 (s, 2H), 7.08 (m, 8H), 2.58 (t, 4H), 1.59 (m, 4H), 1.35 (m, 4H), 0.92 (t, 6H); MS (EI,  $m/e$ ): 348 ( $\text{M}^+$ ), 262 ( $\text{M}^+ - 2\text{C}_3\text{H}_7$ ), 248 ( $\text{M}^+ - \text{C}_3\text{H}_7 - \text{C}_4\text{H}_9$ ), 234 ( $\text{M}^+ - 2\text{C}_4\text{H}_9$ ).

3,4-Bis(4-butylphenyl)thiophene-2,5-diylbismethylene-*N,N*-diethylthiocarbamate (12b). Compound 12b was obtained in an analogous way to that described for 12a. Starting from 9b (730 mg, 2.09 mmol), paraformaldehyde (170 mg, 5.66 mmol), concentrated HCl (1.18 g, 12.0 mmol), and acetic anhydride (2.14 g, 20.9 mmol), 5b was obtained. Without further isolation, 5b was reacted with sodium diethylthiocarbamate trihydrate (1.09 g, 4.84 mmol). The dithiocarbamate monomer 12b was obtained as an orange oil (900 mg, 64% yield);  $^1\text{H NMR}$  ( $\text{CDCl}_3$ ): 7.01–6.94 (AA'BB', 4H), 6.93–6.86 (AA'BB', 4H), 4.63 (s, 4H), 4.01 (q,  $J = 7.2$  Hz, 4H), 3.71 (q,  $J = 7.2$  Hz, 4H), 2.52 (t,  $J = 7.2$  Hz, 4H), 1.53 (q,  $J = 7.2$  Hz, 4H), 1.27 (2t,  $J = 7.2$  Hz, 12H), 0.88 (t,  $J = 7.2$  Hz, 6H);  $^{13}\text{C NMR}$  ( $\text{CDCl}_3$ ): 194.21 (2C), 141.24 (2C), 141.11 (2C), 132.85 (2C), 132.54 (2C), 129.76 (4C), 127.73 (4C), 49.23 (2C), 46.58 (2C), 35.93 (2C), 35.08 (2C), 33.11 (2C), 22.07 (2C), 13.78 (2C), 12.36 (2C), 11.41 (2C).

**Polymerization of 12a (13a).** The polymerization of 12a was performed using three different reaction conditions (cf. entries 1–3, Table 1). A solution of monomer 12a (400 mg, 0.716 mmol) in dry THF (3.6 mL, 0.2 M) at  $-78^\circ\text{C}$  (entries 2 and 3) or  $0^\circ\text{C}$  (entry 1) was degassed for 15 min by passing through a continuous stream of  $\text{N}_2$ , after which LDA (360  $\mu\text{L}$  of a 2 M solution in THF/ $n$ -heptane) was added in one portion. The mixture was kept at  $-78^\circ\text{C}$  (entries 2 and 3) or  $0^\circ\text{C}$  (entry 1) for 90 min, during which time the passing of  $\text{N}_2$  was continued. Subsequently, depending on the polymerization procedure, ethanol (6 mL) was added at  $-78^\circ\text{C}$  to stop the reaction (entry 2) or the solution was allowed to come to  $0^\circ\text{C}$  (entry 3). The reaction mixture was quenched in ice water (100 mL), after which it was neutralized with HCl (1 M in  $\text{H}_2\text{O}$ ). Subsequently, the aqueous phase was extracted with  $\text{CH}_2\text{Cl}_2$  ( $3 \times 60$  mL). The organic layers were combined, after which the solvents were removed by evaporation under reduced pressure. The resulting crude polymer was redissolved in  $\text{CHCl}_3$  (2 mL), and a precipitation was performed in MeOH (100 mL) at  $0^\circ\text{C}$ . The polymer was collected and dried in vacuo and further purified to remove traces of monomer by reprecipitation from diethyl ether/ $n$ -hexane (3:1; 100 mL) at  $0^\circ\text{C}$ . A white solid was obtained (59–117 mg, 20–40% yield).  $^1\text{H NMR}$  ( $\text{CD}_2\text{Cl}_2$ ): 7.21–6.94 (br m, 6H), 6.84–6.60 (br m, 4H), 5.20–5.10 (br s, 1H), 4.10–3.85 (br s, 2H), 3.85–3.55 (br s, 2H), 3.55–3.10 (br s, 2H), 1.42–1.13 (br s, 6H);  $^{13}\text{C NMR}$  ( $\text{CD}_2\text{Cl}_2$ ): 193.40, 140.48, 139.84, 137.81, 136.33 (2C), 135.76, 130.43 (4C), 127.88 (4C), 126.62 (2C), 51.63, 49.25, 47.03, 38.25, 12.89, 11.63. The residual fractions contained low-molecular-weight oligomers and monomer residues.

**Polymerization of 12b (13b).** Compound 13b was obtained in an analogous way to that described for 13a starting from 12b (575 mg, 0.857 mmol) and LDA (429  $\mu\text{L}$  of a 2 M solution in THF/ $n$ -heptane). A white solid was obtained (171 mg, 38% yield).  $^1\text{H NMR}$  ( $\text{CD}_2\text{Cl}_2$ ): 7.01–6.76 (br m, 4H), 6.76–6.53 (br m, 4H), 5.51–5.15 (br s, 1H), 4.14–3.84 (br s, 2H),

**Scheme 3. Synthesis of the Butyl-Substituted 3,4-Diphenylthiophene Monomer 12b and Polymers 13b and 14b:**  
 iv) Pd(PPh<sub>3</sub>)<sub>4</sub>, KF, Toluene/H<sub>2</sub>O; v) CH<sub>2</sub>O, HCl, Ac<sub>2</sub>O; vi) NaSC(S)NEt<sub>2</sub>·3H<sub>2</sub>O, MeOH; vii) LDA, THF; viii) ΔT



3.84–3.54 (br s, 2H), 3.42–3.16 (br s, 2H), 2.63–2.39 (br t, 4H), 1.64–1.40 (br m, 4H), 1.40–1.07 (br m, 10H), 0.99–0.78 (br t, 6H); <sup>13</sup>C NMR (CD<sub>2</sub>Cl<sub>2</sub>): 193.82, 141.48, 140.90 (3C), 137.31, 136.02, 133.78 (2C), 130.45 (4C), 127.81 (4C), 51.87, 49.13, 47.06, 38.30, 35.62 (2C), 33.75 (2C), 22.66 (2C), 14.08 (2C), 12.89, 11.63.

**Thermal Conversion of 13b in Solution (14b).** A solution of **13b** (200 mg) in chlorobenzene (10 mL) was heated to 150 °C and stirred for 20 h. After being cooled to 50 °C, the resulting blue solution was precipitated dropwise in methanol (300 mL). The polymer was filtered off and dried at room temperature under reduced pressure. A black solid was obtained (140 mg, 95% yield); <sup>1</sup>H NMR (CDCl<sub>3</sub>): 7.07–6.92 (m, 4H), 6.92–6.73 (m, 6H), 2.70–2.36 (t, 4H), 1.68–1.41 (m, 4H), 1.41–1.11 (m, 4H), 0.99–0.78 (t, 6H); <sup>13</sup>C NMR (CDCl<sub>3</sub>): 141.88 (2C), 141.40 (2C), 136.52 (2C), 132.58 (2C), 130.41 (4C), 127.82 (4C), 121.80 (2C), 35.35 (2C), 33.30 (2C), 22.28 (2C), 13.99 (2C).

**Thermal Conversion of 13a and 13b in a Thin Film (14a and 14b).** The precursor polymer **13a** or **13b** was spin-coated from a CHCl<sub>3</sub> solution (10 mg/mL) onto NaCl disks at 500 rpm or quartz disks at 700 rpm, respectively. Subsequently, the disks were placed in a thermo cell. A dynamic heating rate of 2 °C/min up to 350 °C under a continuous flow of N<sub>2</sub> was used for the conversion process.

## Results and Discussion

**Monomer Synthesis.** In view of the advantages compared to the Gilch route, the dithiocarbamate precursor route has been chosen as the precursor method of choice to obtain the PTV derivatives (vide supra). The monomers used in the dithiocarbamate precursor route are synthesized from a dihalogenide in a single-step reaction.<sup>7</sup> Three different synthetic routes toward the required dihalogenide, i.e. 3,4-diphenyl-2,5-bis(chloromethyl)thiophene **5a**, have been successfully tested. The first route (Scheme 1) starts with the esterification of the carboxylic groups of commercially available thiodiglycolic acid **1** with ethanol.<sup>16</sup> Next, the Hinsberg reaction between diethyl thiodiacetate **2** and benzil gives the thiophene ring system.<sup>17</sup> Consecutive reduction of the two carboxylic groups of **3** with lithium aluminum hydride (LiAlH<sub>4</sub>) followed by chlorination of the diol with thionyl chloride (SOCl<sub>2</sub>) yields the desired dichloride **5a**. Upon purification by column chromatography (cf. Experimental Section) of **5a** prepared via this first route, some degradation occurred as a result of its instability.

In the second route (Scheme 2, steps i, ii, iii, and v) toward dichloride **5a**, 3,4-diphenylthiophene **9a** has first been dichlorinated via the method developed by Na-

kayama et al.<sup>18,19</sup> The latter involves the synthesis of thiophenes with two substituents on the 3 and 4 positions. Starting from commercially available 2-bromoacetophenone **6**, the reaction with sodium sulfide nonahydrate (Na<sub>2</sub>S·9H<sub>2</sub>O) yields 1,5-diphenyl-3-thiapentane-1,5-dione **7**. Subsequently, 3,4-diphenylthiolane-3,4-diol **8** forms by the intramolecular reductive coupling reaction with a low-valent titanium reagent prepared from titanium(IV) chloride (TiCl<sub>4</sub>) and Zn powder. Treatment of the diol with *p*-toluenesulfonic acid (TsOH·H<sub>2</sub>O) in benzene at reflux temperature gives 3,4-diphenylthiophene **9a**.

The third route (Scheme 2, steps iv and v) also involves the synthesis of **9a**. However, in this route, **9a** is directly synthesized via a Suzuki coupling reaction between the commercially available phenylboronic acid **10a** and 3,4-dibromothiophene **11**. A comparison of the two methods to obtain **9a** reveals that the Suzuki coupling reaction is preferred since it requires only one step and the yield (77%) is better than the overall yield (29%) of the three step synthesis. Having obtained **9a** via the Suzuki coupling, the desired dichloride **5a** is prepared via a typical chloromethylation reaction.<sup>20</sup> It should be noted that **5a** prepared via this route does not require purification by column chromatography, which can lead to degradation (vide supra). Instead, the dithiocarbamate monomer **12a** forms directly from the bis(chloromethyl) compound **5a** by reaction with sodium diethyldithiocarbamate trihydrate.

In view of the better overall monomer yields, the straightforward preparation, and conversion of **5a** without degradation, as well as the lowest number of reaction steps, the third route involving the Suzuki coupling of the phenyl with the thiophene ring has been chosen to prepare **12a**. The overall yield from the starting compounds toward **12a** is 53%. Similar considerations have motivated our choice to prepare the butyl-substituted monomer **12b** only via this route (Scheme 3). This synthesis is straightforward, and the overall yield from the starting compounds toward **12b** is 39%.

**Polymerization.** The polymerization of monomer **12a** has been performed using three different reaction conditions (cf. entries 1–3, Table 1), deviating in the temperatures employed. For monomer **12b**, only one procedure has been selected (cf. entry 4, Table 1). For all reactions, lithium diisopropyl amide (LDA) is used as a base and dried THF as the solvent (Schemes 2 and 3). After the polymerization was allowed to proceed for 90 min, termination of the reaction is achieved by

pouring the polymerization mixture in ice water followed by neutralization with hydrochloric acid to pH = 7. To avoid possible side reactions, the polymerizations performed at  $-78\text{ }^{\circ}\text{C}$  are first quenched with ethanol at  $-78\text{ }^{\circ}\text{C}$  prior to this acidification step (only entries 2 and 4, Table 1). After extraction, the polymers are purified using reprecipitation. The isolated yields range from 20 to 40% (Table 1), with the highest yields being associated with the low polymerization temperatures.

The weight-average molecular weights ( $M_w$ ) of **13a** and **13b** have been determined by analytical SEC in DMF using polystyrene standards. The observed molecular-weight distributions for **13a** are monomodal, with  $M_w$  values ranging from  $24.6 \times 10^3$  to  $50.4 \times 10^3$  and low polydispersities (cf. entries 1–3, Table 1). In contrast, polymer **13b** exhibits a bimodal weight distribution with a lower apparent  $M_w$  ( $M_w = 16.2 \times 10^3$  and  $3.3 \times 10^3$ ; cf. entry 4, Table 1). However, it should be noted that since all molecular weights are referenced to polystyrene standards, the actual value for  $M_w$  will differ from the apparent  $M_w$  observed with analytical SEC.

The electrochemical properties of **13a** and **13b** are typical for nonconjugated polymers, with both the oxidation and the reduction being irreversible. The onset of oxidation in solution is observed at ca. 0.95 V vs Ag/Ag<sup>+</sup> ( $-5.7\text{ eV}$ ) and is associated with the oxidation of the thiophene groups. The onset of reduction is observed at ca.  $-1.3\text{ V}$  vs Ag/Ag<sup>+</sup> ( $-3.5\text{ eV}$ ) and is associated with the dithiocarbamate groups, as well as with impurities.

**Thermal Conversion.** The synthesized precursor polymers can be transferred into the conjugated polymer by a thermal treatment. Upon heating, the dithiocarbamate group of polymer **13a,b** is eliminated to form the corresponding conjugated polymer **14a,b** (Schemes 2 and 3). The thermal conversion can be performed in a thin film or in solution, depending on the type and solubility of the polymer used. Thin-film processes have the added advantage that the thermal elimination reaction and the thermal stability of the polymer can be followed by means of in-situ UV–vis and FT-IR spectroscopy. In this way, one can deduce a reproducible protocol to convert the precursor into the conjugated form, which is essential for applications. The thin-film conversion process was used to obtain both **14a** and **14b**. In contrast to the thin-film elimination, the solution elimination process can be accomplished on a large scale, although this is only of interest when the conjugated polymer obtained is soluble. Hence, the solution elimination was only performed to obtain the butyl-substituted DP-PTV **14b**.

**Formation of 14a in a Thin Film.** Upon heating a thin film of **13a**, the gradual formation of the conjugated structure of polymer **14a** is observed. This is well visible in the temperature-dependent UV–vis absorption spectrum by the development of a band with  $\lambda_{\text{max}} = 550\text{--}600\text{ nm}$  and the decrease of the absorption of **13a** at  $\lambda_{\text{max}} = 247\text{ nm}$  (Figure 1). The thermal process can be better analyzed using the absorbance profiles (Figure 2). In these profiles, an increase in the absorbance at 590 nm can be seen between 110 and 160  $^{\circ}\text{C}$ , reflecting the formation of the conjugated system. Furthermore, in the region between 80 and 160  $^{\circ}\text{C}$ , the formation and disappearance of partially conjugated segments ( $\lambda_{\text{max}} = 403\text{ nm}$ ) is visible. The conversion process is also readily observed using temperature-

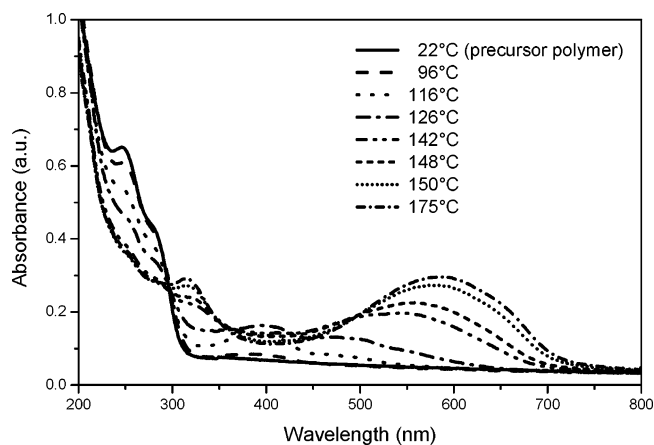


**Figure 1.** Temperature-dependent UV–vis spectra of the elimination of **13a** giving **14a**.

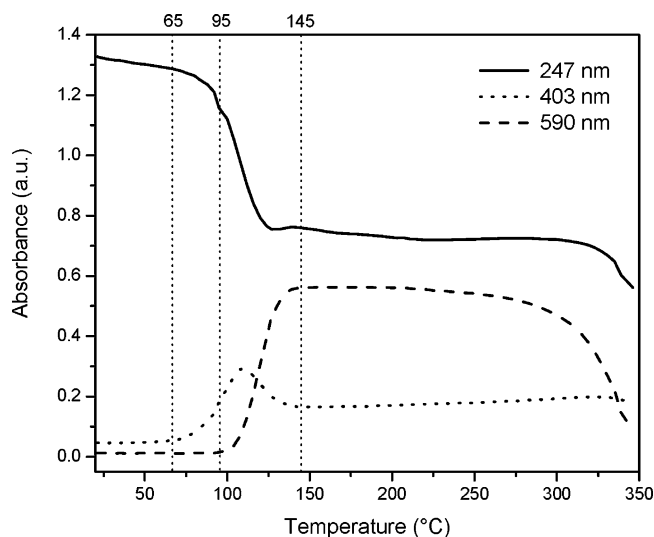


**Figure 2.** UV–vis absorbance profiles at 247, 403, and 590 nm as a function of temperature during the elimination of **13a**.

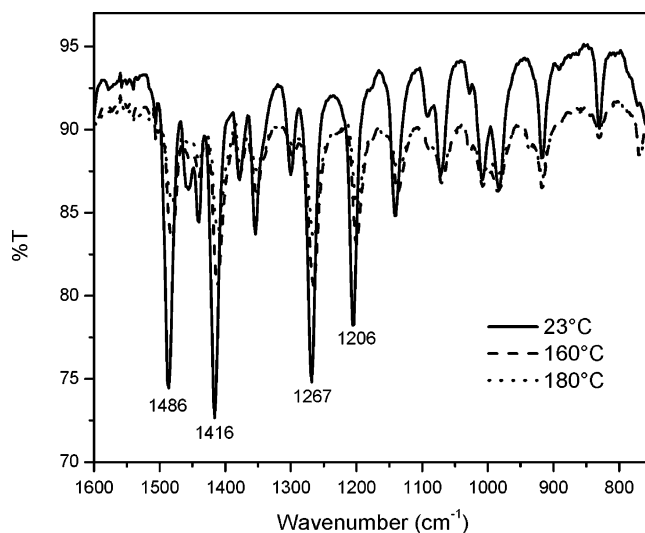


**Figure 3.** Temperature-dependent FT-IR spectra of the elimination of **13a** giving **14a**.

dependent FT-IR spectroscopy (Figure 3). The absorption bands at 1486, 1416, 1267, and 1206  $\text{cm}^{-1}$  all arise from the dithiocarbamate group. From the profiles in Figure 4, it is clear that the increase in double bond absorption ( $934\text{ cm}^{-1}$ ) starts just above 100  $^{\circ}\text{C}$  and the

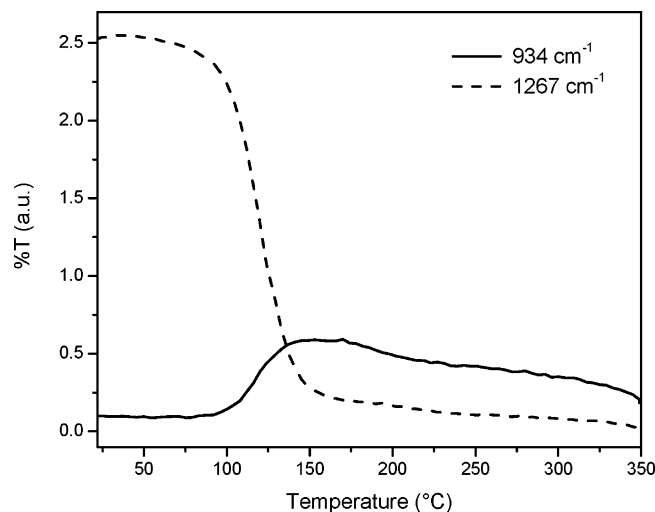


**Figure 4.** IR absorption profiles at 934 and 1267  $\text{cm}^{-1}$  as a function of temperature during the elimination of **13a**.

conversion process is complete around 130 °C for the applied temperature program (heating rate at 2 °C/min). This small difference, as compared to the temperature-dependent UV-vis data, is a result of the increased sensitivity of FT-IR, viz. any double bond formed will be visible in FT-IR, whereas only longer conjugated systems will be visible in the UV-vis. Hence, temperature-dependent FT-IR spectroscopy is an excellent method to study the start and nature of the elimination process, whereas temperature-dependent UV-vis spectroscopy is the most suitable method to determine the end-point of the elimination process. It is noteworthy that the thermal stability of **14a** is 300 °C. This is higher than unsubstituted PTV, which already displays around 275 °C a notable decrease in intensity of the UV-vis absorption maximum.<sup>7</sup>

The room-temperature absorption maximum  $\lambda_{\text{max}}$  of a thin film of **14a** is 600 nm. This is notably higher than  $\lambda_{\text{max}}$  observed by previous researchers for thin films of the same polymer (i.e., 546<sup>13</sup> and 540 nm<sup>14</sup>). These anomalous results are possibly the result of either the presence of polymer defects or the occurrence of incomplete conversion in the previous studies; viz. only comparatively short conjugated systems were present. This is in agreement with our observations in the temperature-dependent UV-vis measurements (Figure 1), in which the  $\lambda_{\text{max}}$  of a thin film of **14a** gradually shifts to higher wavelength upon increase of temperature. In our experiments, all films are heated until no increase of  $\lambda_{\text{max}}$  occurs, i.e., full conjugation is achieved. Upon heating **14a**, a blue-shift of  $\lambda_{\text{max}}$  is observed as a result of the thermochromic effect (175 °C:  $\lambda_{\text{max}} = 590$  nm). This thermochromic shift of 10 nm is smaller than the shift observed for unsubstituted PTV (i.e., 25 nm), possibly reflecting the reduced mobility of the phenyl-substituted PTV main chain.<sup>7</sup> The band gap of **14a** at room temperature can be derived from its UV-vis characteristics by drawing the tangent on the low energetic edge of the absorption spectrum. The intersection with the abscissa is at 730 nm, which corresponds to a band gap of 1.70 eV, which is almost identical to the band gap observed for PTV, i.e., 1.67 eV.<sup>7</sup> Apparently, no reduction in band gap is observed as a result of phenyl substitution, possibly as a result of competing steric effects. In agreement to unsubstituted PTV, as well as other substituted PTV derivatives,<sup>21</sup> thin films

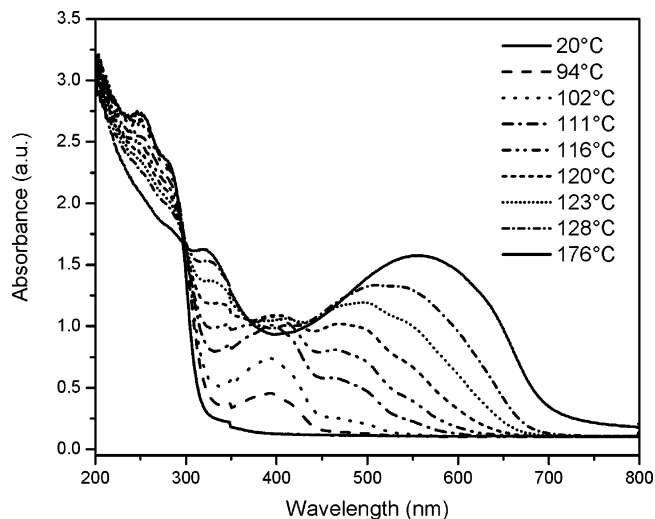


**Figure 5.** Temperature-dependent UV-vis spectra of the elimination of **13b** giving **14b**.

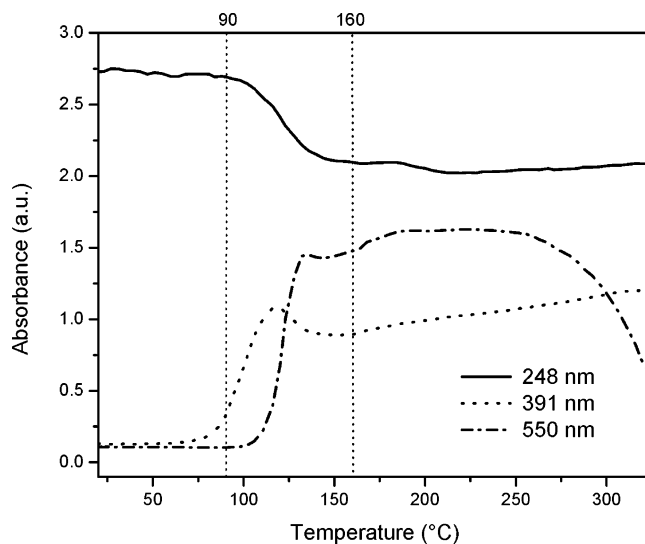


**Figure 6.** UV-vis absorbance profiles at 248, 391, and 550 nm as a function of temperature during the elimination of **13b**.

and solutions of polymer **14a** do not exhibit photoluminescence at room temperature. This is in contrast to copolymers containing PTV repeating units, which do exhibit photoluminescence, although with a low quantum yield.<sup>22</sup>

**Formation of 14b in a Thin Film.** Precursor polymer **13b** was converted in a thin film into **14b** under similar conditions as **13a**. Temperature-dependent UV-vis and FT-IR measurements (Figures 5–8) indicate that the introduction of butyl groups surprisingly has only a small impact on the elimination process, i.e. the elimination process starts at ca. 90 °C. However, it should be noted that the profiles (Figures 6 and 8) indicate that degradation of the conjugated system commences around 275 °C. Apparently, the introduction of the butyl side chains somewhat reduces the thermal stability. Notwithstanding, thermal stability up to 275 °C is sufficiently high for virtually all applications.

The introduction of alkyl side chains has also an impact on the UV-vis absorption properties. The room-temperature absorption maximum,  $\lambda_{\text{max}}$ , of a thin film of **14b** is 590 nm, which is slightly blue-shifted with respect to the absorption maximum observed for **14a**. This shift is also observed for the band gap. The low

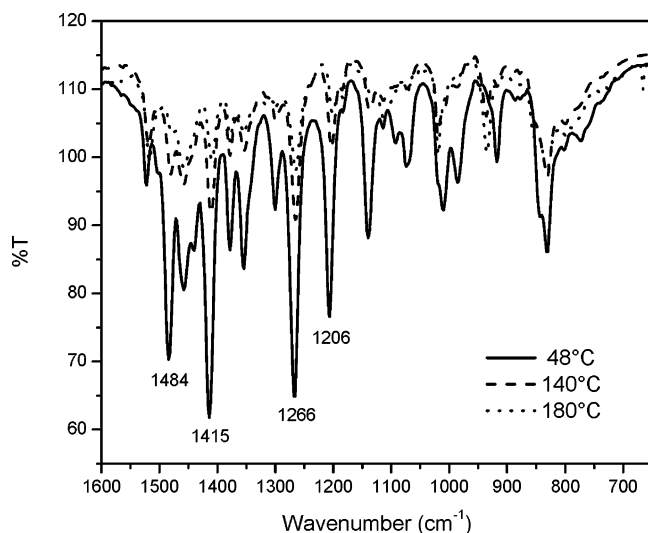


**Figure 7.** Temperature-dependent FT-IR spectra of the elimination of **13b** giving **14b**.

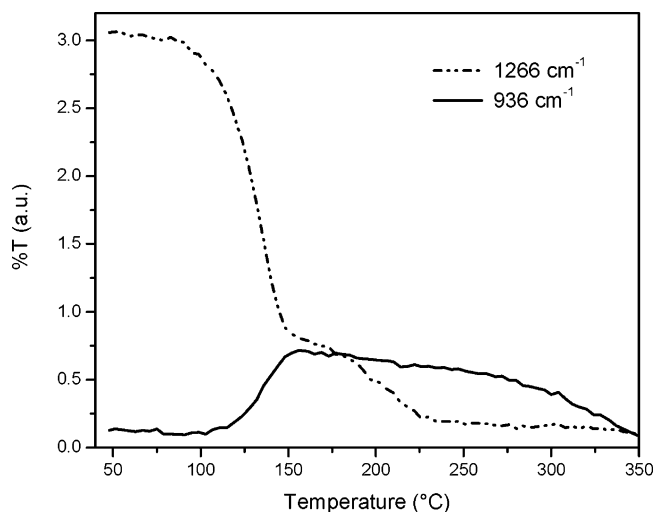


**Figure 8.** IR absorption profiles at 936 and 1266  $\text{cm}^{-1}$  as a function of temperature during the elimination of **13b**.

energetic edge of the absorption spectrum of **14b** is at 701 nm, which corresponds to a band gap of 1.77 eV. This increase in band gap, as compared to **14a**, is opposite to what can be expected for the introduction of lightly electron donating substituents. Apparently, the effect of the reduced electronic interchain interactions, as well as the increased disorder in the conjugated system created by the introduction of the alkyl side chains, is larger than the possible electronic substituent effects.

**Formation of 14b in Solution.** In addition to the thin-film conversion (vide supra), highly soluble **13b** has also been converted into **14b** in solution. Chlorobenzene was used as the solvent, and the process was heated to 150 °C (cf. Experimental Section). The solution conversion process is virtually quantitative (yield: 95%). The optical properties of **14b** prepared in solution are identical to those found for **14b** prepared in the thin-film process. It is noteworthy that **14b** is soluble in a wide variety of common organic solvents, including  $\text{CHCl}_3$ ,  $\text{CH}_2\text{Cl}_2$ , THF, toluene, and chlorobenzene. Hence, **14b** can be analyzed in solution, as well as spin-coated from a solution, thus considerably increasing the applicability of this polymer for electronic applications.

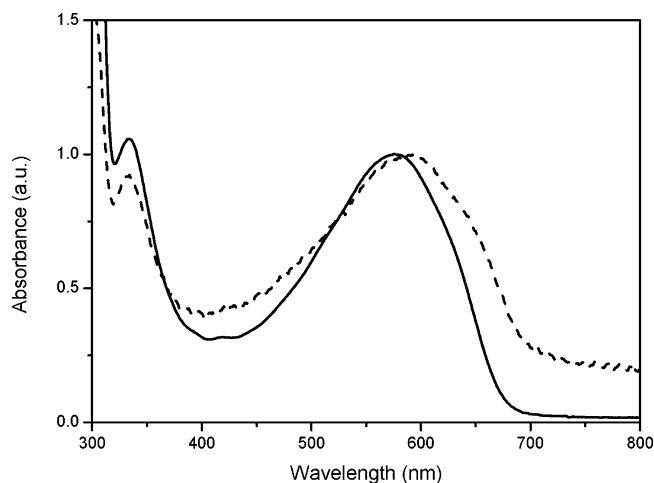


**Figure 9.** UV-vis absorption spectra of **14b** in a  $\text{CHCl}_3$  solution (solid) and as a thin film spin-coated from a  $\text{CHCl}_3$  solution (dashed).

The apparent molecular weight ( $M_w$ ) observed with analytical SEC of **14b** prepared in this way is  $9.0 \times 10^3$  (solvent, THF; polydispersity, PD = 1.7). The observed absorption maximum ( $\lambda_{\text{max}}$ ) of a thin film of **14b** spin-coated from a  $\text{CHCl}_3$  solution is 592 nm. The UV-vis absorption spectrum of a solution of **14b** in  $\text{CHCl}_3$  exhibits an absorption maximum  $\lambda_{\text{max}} = 577$  nm (Figure 9). This is 15 nm blue-shifted with respect to the absorption maximum of a thin film of **14b** as a result of electronic interchain interactions in the solid state. Similarly to **14a**, solutions and thin-film polymer **14b** do not exhibit photoluminescence at room temperature (vide supra). The stability of spin-coated thin films of **14b** formed in solution was investigated using temperature-dependent UV-vis spectroscopy. The onset of degradation occurs around 180 °C, as compared to 275 °C in the films of **14b** formed directly in a thin film. The origin of this difference is not certain but may be related to the exposure of the solution-formed **14b** to ambient conditions after synthesis and during spin-coating.

**Electrochemistry.** Cyclic voltammetry (CV) was employed to investigate the electrochemical behavior of polymers **14a** and **14b** and to estimate their highest occupied molecular orbital (HOMO) energy levels. The cyclic voltammograms of **14a** and **14b** display distinct oxidation and reduction processes (Figure 10). Whereas the oxidation process is directly associated with the conjugated structure, i.e. p-doping, the reduction process is irreversible, poorly defined, and associated with polymer defects and traces of impurities. A similar reduction behavior was observed for the precursor polymers **13a** and **13b**. Hence, no n-doping has been observed. In contrast, the observed p-doping process is fully reversible. The oxidation potential of **14a** is 0.41 V vs  $\text{Ag}/\text{Ag}^+$ . However, the HOMO energy level is more accurately determined from the onset of oxidation. In the anodic scan, the onset of oxidation of **14a** occurs at 0.19 V vs  $\text{Ag}/\text{Ag}^+$ , which corresponds to a HOMO energy level of  $-4.89$  eV. The p-doping for **14b** is also reversible (oxidation potential 0.46 V vs  $\text{Ag}/\text{Ag}^+$ ), although not as well defined as for **14a**. The onset of oxidation of **14b** occurs at 0.30 V vs  $\text{Ag}/\text{Ag}^+$ , which corresponds to a HOMO energy level of  $-5.00$  eV. For comparison, the oxidation potential of PTV is 0.39 V vs  $\text{Ag}/\text{Ag}^+$  with an onset of oxidation at 0.08 V vs  $\text{Ag}/\text{Ag}^+$ , which corresponds to a HOMO energy level of  $-4.78$  eV. The shift

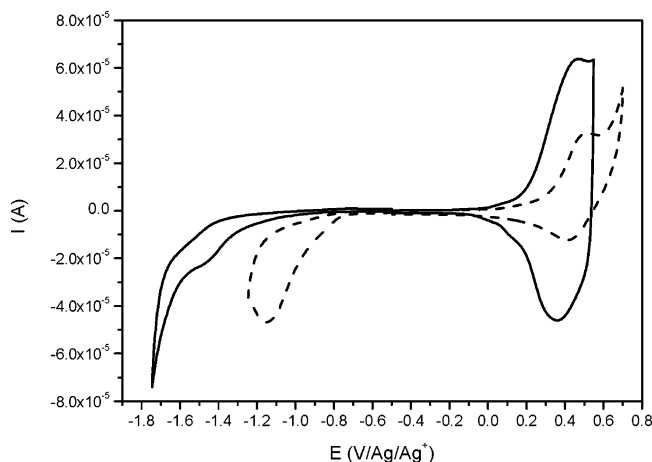


**Figure 10.** Cyclic voltammograms of the oxidation and reduction behavior of thin films of **14a** (solid) and **14b** (dashed).

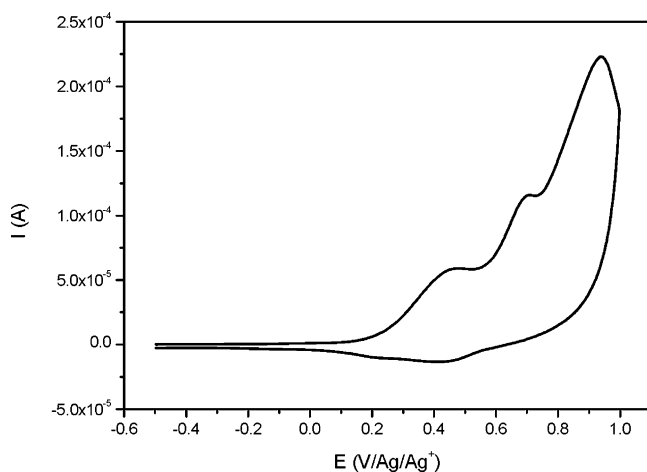


**Figure 11.** Cyclic voltammogram of the oxidation behavior of a thin film of **14a**.

of the HOMO energy level in going from unsubstituted **14a** to butyl-substituted **14b** partially corresponds to the change in band gap observed with UV-vis spectroscopy (vide supra). Combining of the electrochemical data and the UV-vis characteristics gives an estimate of the LUMO energy levels of **14a** and **14b**, i.e.  $-3.19$  eV and  $-3.23$  eV, respectively.

It should be noted that the oxidation process can also be observed visually. For both **14a** and **14b**, a color change of the films from blue to light yellow was observed upon oxidation. Subsequently, in the reverse process upon dedoping, the color of the film returned to blue. This observation further confirms the reversibility of the p-doping process. It is noteworthy that, upon application of increased bias (i.e., scanning to 1.0 V vs Ag/Ag<sup>+</sup>), a second and a third oxidation process can be observed for **14a** (Figure 11). Similarly to the first oxidation process, which is associated with the HOMO energy level, the second oxidation process with an oxidation potential of ca. 0.7 V vs Ag/Ag<sup>+</sup> ( $-5.4$  eV) is reversible. This process is possibly associated with the oxidation of the phenyl rings. In contrast, the third oxidation process with an oxidation potential of ca. 0.9 V vs Ag/Ag<sup>+</sup> ( $-5.6$  eV) is irreversible and results in the irreversible degradation of the conjugated system.

## Conclusions

In conclusion, the synthesis of DP-PTV derivatives via the dithiocarbamate precursor route has been demon-

strated. The monomer preparation procedures have been optimized and DP-PTV **14a** is readily accessible. As a result of the introduction of phenyl substituents, **14a** demonstrates an enhanced thermal stability as compared to PTV. Furthermore, **14a** exhibits a significantly improved  $\lambda_{\max}$  value as compared to previous reports, indicating its improved purity and lower defect levels. In addition to DP-PTV, a novel dibutyl-substituted DP-PTV **14b** has been prepared, which is soluble in common organic solvents. This allows the solution processing of DP-PTV derivatives for applications. Both polymers have a low band gap (1.7–1.8 eV) and can be reversibly p-doped.

**Acknowledgment.** The authors gratefully acknowledge The Fund for Scientific Research-Flanders (FWO) and the Belgian Program on Interuniversity Attraction Poles (IUAP), initiated by the Belgian State Prime Minister's Office, for the financial support. We also want to thank the IWT (Institute for the Promotion of Innovation by Science and Technology in Flanders) for the financial support via the SBO-project 030220 "Nanosolar". K.C. wishes to thank the IUAP-V and S.F. the BOF-LUC for granting a Ph.D. fellowship.

## References and Notes

- (1) Kraft, A.; Grimsdale, A. C.; Holmes, A. B. *Angew. Chem., Int. Ed.* **1998**, *37*, 403.
- (2) Dimitrakopoulos, C. D.; Mascaro, D. J. *IBM J. Res. Dev.* **2001**, *45*, 1, 11.
- (3) Nunzi, J.-M. *C. R. Physique* **2002**, *3*, 523.
- (4) Fuchigami, H.; Tsumura, A.; Koezuka, H. *Appl. Phys. Lett.* **1993**, *63*, 10, 1372.
- (5) Brown, A. R.; Jarrett, C. P.; de Leeuw, D.; Matters, M. *Synth. Met.* **1997**, *88*, 37.
- (6) Vandamme, L. K. J.; Feyaerts, R.; Trefan, G.; Detcheverry, C. *J. Appl. Phys.* **2002**, *91*, 2, 719.
- (7) Henckens, A.; Lutsen, L.; Vanderzande, D.; Knipper, M.; Manca, J.; Aernouts, T.; Poortmans, J. *SPIE Proc.* **2004**, 26–30 April, Strasbourg, France.
- (8) Dhanabalan, A.; van Duren, J. K. J.; van Hal, P. A.; van Dongen, J. L. J.; Janssen, R. A. J. *Adv. Funct. Mater.* **2001**, *11*, 4, 255.
- (9) Winder, C.; Mühlbacher, D.; Neugebauer, H.; Sariciftci, N. S.; Brabec, C. J.; Janssen, R. A. J.; Hummelen, J. C. *Mol. Cryst. Liq. Cryst.* **2002**, *385*, 93.
- (10) Wei, P. K.; Hsu, J. H.; Hsieh, B. R.; Fann, W. S. *Adv. Mater.* **1996**, *8*, 7, 573.
- (11) Wei, P. K.; Hsu, J. H.; Fann, W. S.; Hsieh, B. R. *Polym. Mater. Sci. Engin.* **1996**, *75*, 325.
- (12) Wei, P. K.; Hsu, J. H.; Fann, W. S.; Hsieh, B. R. *Synth. Met.* **1997**, *85*, 1421.
- (13) Hsieh, B. R.; Johnson, G. E.; Antoniadis, H.; McGrane, K. M.; Stolka, M. U.S. Patent 5,558,904, 1996.
- (14) Tan, C. H.; Inigo, A. R.; Hsu, J. H.; Fann, W. S.; Wei, P. K. *J. Phys. Chem. Solids* **2001**, *62*, 1643–1654.
- (15) Cheng, H.; Elsenbaumer, R. L. *J. Chem. Soc., Chem. Commun.* **1995**, 1451.
- (16) Sankaran, B.; Reynolds, J. R. *Macromolecules* **1997**, *30*, 9, 2582.
- (17) Hinsberg, O. *Chem. Ber.* **1910**, *43*, 901.
- (18) Nakayama, J.; Hasemi, R. *J. Am. Chem. Soc.* **1990**, *112*, 5654.
- (19) Nakayama, J.; Hasemi, R.; Yoshimura, K.; Sugihara, Y.; Yamaoka, S. *J. Org. Chem.* **1998**, *63*, 4912.
- (20) Becker, H.; Spreitzer, H.; Ibrom, K.; Kreuder, W. *Macromolecules* **1999**, *32*, 4925.
- (21) Goldini, F.; Janssen, R. A. J.; Meijer, E. W. *J. Polym. Sci., Part A: Polym. Chem.* **1999**, *37*, 4629.
- (22) Chen, B.; Wu, Y.; Wang, M.; Wang, S.; Sheng, S.; Zhu, W.; Sun, R.; Tian, H. *Eur. Polym. J.* **2004**, *40*, 6, 1183–1191.